JNeurosci
THE JOURNAL OF NEUROSCIENCE

Research Articles: Neurobiology of Disease

Hyperactivity of anterior cingulate cortex areas 24a/24b drives chronic pain-induced anxiodepressive-like consequences

Jim Sellmeijer[1,2,3,4], Victor Mathis[1], Sylvain Hugel[1], Xu-Hui Li[6], Qian Song[6], Qi-Yu Chen[6], Florent Barthas[1,2], Pierre-Eric Lutz[1], Meltem Karatas[1,2], Andreas Luthi[3], Pierre Veinante[1,2], Michel Barrot[1], Min Zhuo[5,6] and Ipek Yalcin[1]

[1]*Institut des Neurosciences Cellulaires et Intégratives, Centre National de la Recherche Scientifique, 67084 Strasbourg, France*

[2]*Université de Strasbourg, 67084 Strasbourg, France*

[3]*Friedrich Miescher Institute for Biomedical Research, 4058 Basel, Switzerland*

[4]*Faculty of Biology and Bernstein Center Freiburg, University of Freiburg, D-79104 Freiburg, Germany*

[5]*Department of Physiology, Faculty of Medicine, University of Toronto, 1 King's College Circle, Toronto, Ontario, M5S 1A8, Canada*

[6]*Center for Neuron and Brain Disease, Frontier Institutes of Science and Technology, Xi'an Jiaotong University, Xi'an, 710049, China*

DOI: 10.1523/JNEUROSCI.3195-17.2018

Received: 7 November 2017

Revised: 10 January 2018

Accepted: 10 February 2018

Published: 20 February 2018

Author contributions: J.S., V.M., S.H., X.-H.L., Q.S., Q.-Y.C., F.B., M.K., and I.Y.-C. performed research; J.S., S.H., X.-H.L., Q.S., Q.-Y.C., F.B., P.-E.L., P.V., A.A., M.Z., and I.Y.-C. analyzed data; J.S. and I.Y.-C. wrote the paper; A.L., A.A., M.B., M.Z., and I.Y.-C. designed research.

Conflict of Interest: The authors declare no competing financial interests.

We thank Stéphane Doridot for assistance in breeding mice and in genotyping and Elaine Gravel for her technical support. We also thank Dr. Modesto R Peralta for English editing. This work was supported by the Centre National de la Recherche Scientifique (contract UPR3212), the University of Strasbourg, the NeuroTime Erasmus Mundus Joint doctorate and by a NARSAD Young Investigator Grant (18893) from the Brain & Behavior Research Foundation (IY). PEL was supported by fellowships from the Fondation pour la Recherche Médicale, and from the Fondation Deniker. MZ was supported by Canada Research Chair, CIHR Operating Grant MOP-124807 and Azrieli Neurodevelopmental Research Program and Brain Canada.

Address correspondence to Ipek Yalcin, Institut des Neurosciences Cellulaires et Intégratives, UPR3212 CNRS, 5 rue Blaise Pascal, 67084 Strasbourg cedex, France. Phone: (33) 3 88 45 66 28; E-mail: yalcin@inci-cnrs.unistra.fr

Cite as: J. Neurosci ; 10.1523/JNEUROSCI.3195-17.2018

Title Page

Hyperactivity of anterior cingulate cortex areas 24a/24b drives chronic pain-induced anxiodepressive-like consequences

Running title: Cortex in chronic pain-induced depression

Jim Sellmeijer[1,2,3,4], Victor Mathis[1], Sylvain Hugel[1], Xu-Hui Li[6], Qian Song[6], Qi-Yu Chen[6], Florent Barthas[1,2], Pierre-Eric Lutz[1], Meltem Karatas[1,2], Andreas Luthi[3], Pierre Veinante[1,2], Ad Aertsen[4], Michel Barrot[1], Min Zhuo[5,6], Ipek Yalcin[1]

1. Institut des Neurosciences Cellulaires et Intégratives, Centre National de la Recherche Scientifique, 67084 Strasbourg, France
2. Université de Strasbourg, 67084 Strasbourg, France
3. Friedrich Miescher Institute for Biomedical Research, 4058 Basel, Switzerland
4. Faculty of Biology and Bernstein Center Freiburg, University of Freiburg, D-79104 Freiburg, Germany
5. Department of Physiology, Faculty of Medicine, University of Toronto, 1 King's College Circle, Toronto, Ontario, M5S 1A8, Canada,
6. Center for Neuron and Brain Disease, Frontier Institutes of Science and Technology, Xi'an Jiaotong University, Xi'an, 710049, China

Address correspondence to Ipek Yalcin, Institut des Neurosciences Cellulaires et Intégratives, UPR3212 CNRS, 5 rue Blaise Pascal, 67084 Strasbourg cedex, France. Phone: (33) 3 88 45 66 28; E-mail: yalcin@inci-cnrs.unistra.fr

Number of pages: 32

Number of figures: 7

Number of tables: 0

Number of words Abstract: 153, Introduction: 650, Discussion: 1500

Acknowledgement: We thank Stéphane Doridot for assistance in breeding mice and in genotyping and Elaine Gravel for her technical support. We also thank Dr. Modesto R Peralta for English editing. This work was supported by the Centre National de la Recherche Scientifique (contract UPR3212), the University of Strasbourg, the NeuroTime Erasmus Mundus Joint doctorate and by a NARSAD Young Investigator Grant (18893) from the Brain & Behavior Research Foundation (IY). PEL was supported by fellowships from the Fondation pour la Recherche Médicale, and from the Fondation Deniker. MZ was supported by Canada Research Chair, CIHR Operating Grant MOP-124807 and Azrieli Neurodevelopmental Research Program and Brain Canada.

The authors declare no competing financial interests.

Abstract

Pain associates both sensory and emotional aversive components, and often leads to anxiety and depression when it becomes chronic. Here, we characterized, in a mouse model, the long-term development of these sensory and aversive components as well as anxiodepressive-like consequences of neuropathic pain and determined their electrophysiological impact on the anterior cingulate cortex (ACC, cortical areas 24a/24b). We show that these symptoms of neuropathic pain evolve and recover in different time courses following nerve injury in male mice. *In vivo* electrophysiological recordings evidence an increased firing rate and bursting activity within the ACC when anxiodepressive-like consequences developed and this hyperactivity persists beyond the period of mechanical hypersensitivity. Whole-cell patch-clamp recordings also support ACC hyperactivity, as shown by increased excitatory postsynaptic transmission and contribution of NMDA receptors. Optogenetic inhibition of the ACC hyperactivity was sufficient to alleviate the aversive and anxiodepressive-like consequences of neuropathic pain, indicating that these consequences are underpinned by ACC hyperactivity.

Significance Statement

Chronic pain is frequently comorbid with mood disorders such as anxiety and depression. It has been shown that it is possible to model this comorbidity in animal models by taking into consideration the time factor. In this study, we aimed at determining the dynamic of different components and consequences of chronic pain, and correlated them with electrophysiological alterations. By combining electrophysiological, optogenetic and behavioral analyses in a mouse model of neuropathic pain, we show that the mechanical hypersensitivity, ongoing pain, anxiodepressive-consequences and their recoveries do not necessarily exhibit temporal synchrony during chronic pain processing, and that the hyperactivity of the anterior cingulate cortex is essential for driving the emotional impact of neuropathic pain.

Introduction

Mood disorders, such as anxiety and depression, are frequently observed in patients suffering from chronic pain, which adds dramatically to the patients' pain burden (Radat et al., 2013). Preclinical studies have shown that the anxiodepressive-like consequences of chronic pain, like in neuropathic pain condition, can be studied in murine models (Narita et al., 2006; Yalcin et al., 2011; Alba-Delgado et al., 2013) and further highlight the importance of the time factor in the development of these consequences (Yalcin et al., 2011; Barthas et al., 2015). It has been recently shown that depressive-like behaviors are still present 2 weeks after recovery from mechanical hypersensitivity in an animal model of neuropathic pain (Dimitrov et al., 2014), raising the question of whether these consequences of chronic pain might be maintained in the long-term independently from sensory aspects.

The anterior cingulate cortex (ACC) is involved in the processing of both pain and mood-related information (Shackman et al., 2011; Bliss et al., 2016). The implication of the ACC in depression is supported by a hyperactivity of the ACC in depressed patients (Mayberg et al., 1999; Drevets et al., 2002; Yoshimura et al., 2010), and by changes in the mouse ACC transcriptome that are correlated with depressive-like behaviors in the chronic stress model (Surget et al., 2009). Clinical imaging studies also show the recruitment of the ACC in pain processing (Peyron et al., 2000), and preclinical studies more precisely associate the activation of ACC neurons with pain-like aversive (Johansen et al., 2001; Barthas et al., 2015) or fearful (Tang et al., 2005) behaviors. Potentiation of synaptic responses (Xu et al., 2008; Chen et al., 2014), disinhibition (Blom et al., 2014) and increased excitability (Li et al., 2010; Cordeiro Matos et al., 2015) are also observed *ex vivo* in the ACC in rodent models of chronic pain. *In vivo* studies further show that a lesion of the ACC prevents both chronic pain-induced anxiodepressive-like behaviors (Barthas et al., 2015) and the aversiveness of ongoing pain (Johansen et al., 2001; King

et al., 2009; Qu et al., 2011; Barthas et al., 2015). In addition, it has been reported that (i) optogenetic activation of pyramidal neurons within the ACC is sufficient to induce anxiodepressive-like behaviors in naive mice (Barthas et al., 2015) and that (ii) these behaviors are associated with transcriptomic changes in the ACC (Barthas et al., 2017). Finally, presynaptic long-term potentiation in the ACC has been linked to pain-related anxiety (Koga et al., 2015).

Accordingly, the ACC seems to be a critical brain region implicated in different symptoms of chronic pain, and especially in its anxiodepressive-like consequences (Barthas et al., 2015; Koga et al., 2015).

In the present study, we first aimed at characterizing the long-term evolution, over 6 months, of mechanical hypersensivity, of the aversive state induced by ongoing pain and of the anxiodepressive-like consequences of neuropathic pain in mice using the "cuff" model. This model, based on sciatic nerve cuffing, has the advantage of displaying spontaneous recovery from mechanical allodynia (Yalcin et al., 2014b), which allows studying the behavioral consequences of neuropathic pain in the presence and absence of hypersensitivity. We also determined the time-course of *in vivo* electrophysiological alterations accompanying these various symptoms within the ACC (cortical areas 24a/24b, (Fillinger et al., 2017b)), and correlated them to the different stages of the pathology.

This long-term characterization evidenced that the mechanical hypersensitivity, the aversiveness of ongoing pain and the anxiety/depressive-like consequences of neuropathic pain evolve in distinct time courses. The *in vivo* electrophysiological recordings further showed a correlation between ACC hyperactivity and the aversive and anxiodepressive-like consequences. These results are reinforced by whole-cell patch-clamp recordings highlighting a facilitation of excitatory synaptic transmission onto ACC pyramidal neurons in cuff implanted animals showing depressive-like consequences. Moreover, we showed that optogenetic inhibition of the ACC was

sufficient to counteract the chronic pain-induced emotional consequences, which supports a causal link between ACC hyperactivity and the emotional aspects of neuropathic pain.

Material and Methods

ANIMALS

Experiments were conducted using male adult C57BL/6J (RRID:IMSR_JAX:000664) mice (Charles River, L'Arbresle, France), group-housed with a maximum of five animals per cage and kept under a reversed 12-hour light/dark cycle. Only the animals used for optogenetic experiments were single housed after the optic fiber implantation to avoid possible damage to the implant. Behavioral tests were conducted during the dark phase under red light. The Chronobiotron animal facilities are registered for animal experimentation (Agreement A67-2018-38) and protocols were approved by the local ethical committee of the University of Strasbourg (CREMEAS, nº 02015021314412082).

SURGICAL PROCEDURES

Surgical procedures were performed under ketamine/xylazine anesthesia (ketamine 17 mg/ml, xylazine 2.5 mg/ml; intraperitoneal, 4 ml/kg) (Centravet, Taden, France).

Neuropathic pain model. Neuropathic pain was induced by implanting a 2 mm section of PE-20 polyethylene tubing (Harvard Apparatus, Les Ulis, France) around the main branch of the right sciatic nerve (Benbouzid et al., 2008; Barrot, 2012; Yalcin et al., 2014b). Before surgery, animals were assigned to experimental groups according to their initial mechanical nociceptive threshold, in order to even out the average mechanical threshold among groups. Animals in the sham condition underwent the same procedure without cuff implantation.

134

135 *Virus injection.* After anesthesia, C57BL/6J mice were placed in a stereotaxic frame (Kopf,
136 Tujunga, CA). 0.5 µl of AAV5-CaMKIIa-eArchT3.0-EYFP (UNC Vector core) was injected
137 bilaterally in the ACC (areas 24a/24b) using a 5 µl Hamilton syringe (0.05 µl/minute, coordinates
138 for the ACC: +0.7 mm from bregma, lateral: ±0.3 mm, dorsoventral: -1.5 mm from the skull).
139 After injection, the 32 gauge needle remained in place for 10 minutes and then the skin was
140 sutured.

141

142 *Optic fiber cannula implantation.* Four weeks after virus injection, the animals underwent optic
143 fiber cannula implantation. The mice were implanted unilaterally over the site of virus injection.
144 Cannulas were implanted in the left hemisphere in half of each experimental group, whereas the
145 other half received the implant in the right hemisphere. The optic fiber cannula was 1.7 mm long
146 and 220 µm in diameter. The cannula was inserted 1.5 mm deep in the brain (MFC_220/250-
147 0.66_1.7mm_RM3_FLT, Doric Lenses) (Barthas et al., 2015).

148

149 **Optogenetic procedures**

150 After a 3 to 7 days recovery period, we performed behavioral experiments. Green laser light
151 (custom assembly, Green 520 nm, 16 mW, Miniature Fiber Coupled Laser Diode Module, Doric
152 Lenses) was delivered through a 0.75 m long monofiber optic patch chord (MFP_240/250/2000-
153 0.63_0.75m_FC-CM3, Doric Lenses) that was mounted to the optic fiber implant on the skull.
154 Optogenetic inhibition was performed either before or during behavioral testing, by continuous
155 light for 5 minutes with a power of 16 mW. Control animals underwent the same procedures but
156 the light was turned off during stimulation protocols.

157

158 **Behavioral analysis**

159 Behavioral testing was performed during the dark phase, under red light. While each mouse went
160 through different tests, those were conducted according to the following rules: excepted for the
161 von Frey results, no mouse went twice through the same test (i.e. the different time-points for a
162 given test were performed on independent sets of animals); the forced swim test was always
163 considered as terminal (i.e. no other test was done on mice after they went through forced
164 swimming). Each graph displayed in Figure 2 is from a given (single) batch of animals, with
165 Sham and Cuff mice from this batch tested on the same day(s) to always ensure internal control,
166 and with von Frey data always available the same week for these mice. Thus, for this general
167 characterization, we did not mix results from different batches within a given graph of Figure 2,
168 and we always had the hypersensitivity status of the animals to justify the hypersensitivity
169 component of the time point (TP) clustering. Mechanical threshold and anxiodepressive-like
170 behaviors of animals used for electrophysiology studies were determined before recordings.
171 *Nociceptive testing.* Von Frey filaments were used to determine the mechanical threshold of
172 hindpaw withdrawal (Bioseb, Chaville, France). Mice were placed in Plexiglas® boxes (7 cm x 9
173 cm x 7 cm) on an elevated mesh screen. After 15 minute habituation, animals were tested by
174 applying a series of ascending forces (0.16 to 8 grams) on the plantar surface of each hind paw.
175 Each filament was tested 5 times per paw, applied until it just bent (Yalcin et al., 2014b; Barthas
176 et al., 2015). The threshold was defined as 3 or more withdrawals observed out of the 5 trials. In
177 order to characterize changes in mechanical thresholds during an extended period, we tested
178 animals before and at given time points after sciatic nerve surgery. The animals used for
179 optogenetic inhibition of the ACC were tested before sciatic nerve surgery and before the
180 behavioral tests. Finally, we tested the animals during light stimulation to see whether
181 optogenetic inhibition affected mechanical thresholds.

182

183 *Conditioned place preference.* To test the motivational drives resulting from the aversive state
184 induced by ongoing pain and from its relief by clonidine, a single trial conditioned place
185 preference (CPP) paradigm was used (King et al., 2009). In this test, animals develop a
186 preference to a clonidine-paired chamber due to both pain relief in this environment and
187 avoidance for the saline-paired chamber associated with ongoing pain. The apparatus consisted of
188 3 Plexiglas® chambers separated by manually operated doors (Imetronic, Pessac, France). Two
189 chambers (15cm x 24cm x 33cm), distinguished by the texture of the floor and by the wall
190 patterns, were connected by a central chamber (15cm x 11cm x 33cm). Animals went through a
191 3-day preconditioning period during which they had access to all chambers for 30 minutes each
192 day. Time spent in each chamber was analyzed to control for the lack of preference for one of the
193 chambers. Animals spending more than 75% or less than 25% of the total time in one of the
194 chambers were excluded from the study. On the conditioning day (day 4), mice first received
195 intrathecal saline (10 µl) and were placed in a conditioning chamber. Four hours later, mice
196 received clonidine (10 µg/10 µl), an α2-adrenoceptor agonist inducing analgesia after intrathecal
197 administration, and were placed in the opposite chamber. Conditioning lasted 15 min per
198 chamber, without allowing the animal to access the other chambers. On the fifth day, mice were
199 placed in the center chamber, with free access to both conditioning chambers and the time spent
200 in each chamber was recorded for 30 min. CPP was assessed in separate sets of mice
201 corresponding (in weeks, W) to 8 W (TP2), 14 W (TP3) and 22 W (TP4) after cuff implantation.
202 The exact TP status of the animals was each time determined by using the von Frey test for
203 mechanical hypersensitivity and by using the novelty suppressed feeding test for the
204 anxiodepressive-like state.

To study whether optogenetic inhibition of the ACC caused a preference, we used another version of the CPP test, with a custom made box with 2 chambers (23cm x 22cm x 16cm), distinguishable by different wall patterns, and connected to each other by a single sliding door. The test lasted four days. On the first day, animals were habituated to the testing box by allowing them full access to both compartments for 5 min. During the second and third days, animals went through a conditioning period. For this purpose, during the mornings, the animals were placed in the compartment where they received no light stimulation, whereas during the afternoon sessions the animals were light-stimulated following the above mentioned protocol. Control animals underwent the same procedures, but during the afternoon session the laser light remained off. On the fourth day we placed the animal at the level of the sliding door and measured the time spent in each compartment during 5 minutes.

Dark-light test. To measure anxiety-like behavior, we performed the dark-light test (Vogt et al., 2016), with a two compartment testing box (18cm x 18cm x 14.5cm) connected by a dark tunnel (8.5cm x 7cm x 6cm). One compartment was brightly illuminated (1500 lux) whereas the other was dark. Mice were placed in the dark compartment at the beginning of the test and the time spent in the lit compartment was recorded for 5 min. This test was performed 2, 8, 11 and 15 W after sciatic nerve surgery in different sets of animals.

Novelty suppressed feeding test. The novelty suppressed feeding (NSF) test was used to assess anxiodepressive-like behavior as it induces a conflict between the drive to eat and the fear of venturing into the center of the box (Yalcin et al., 2011; Barthas et al., 2015; Barthas et al., 2017). For this test, we used a plastic box with the floor covered with 2 cm of sawdust. Animals were food deprived for 24h. At the time of testing, a single pellet of food was placed in the middle of

the testing chamber under 7 lux, and the latency to eat the pellet was recorded within a 5 minute period. The NSF test was performed 2, 8, 11, 16, 18 and 21 W after sciatic nerve surgery in independent sets of animals. For the optogenetic experiment, the NSF test was performed immediately after the inhibition procedure.

Splash test. This test was used to measure grooming behavior indirectly (Yalcin et al., 2011; Barthas et al., 2015), since decreased grooming can be related to the loss of interest in performing self-relevant tasks. This behavior was measured for 5 minutes after spraying a 10% sucrose solution on the coat of the animals. The splash test was performed on animals 3, 9, 12, 14 and 16 W after the peripheral nerve injury in independent sets of animals. For the optogenetic experiment, the splash test was performed during the inhibition procedure.

Forced swimming test (FST). This test was performed to evaluate despair-like behavior (Porsolt et al., 1977). We lowered the mouse into a glass cylinder (height 17.5 cm, diameter 12.5 cm) containing 11.5 cm of water (23-25°C). The test duration was 6 minutes, but since only little immobility was observed during the first 2 minutes, we only quantified the duration of immobility during the last 4 minutes of the test. We considered the mouse to be immobile when it floated upright in the water, with only minor movements to keep its head above the water. This test was performed 7, 14, 17, 18 and 21 W after the sciatic nerve surgery in different sets of animals.

Locomotor activity. At three different time points, locomotor activity was monitored in both sham and cuff-implanted mice. Mice were individually placed in activity cages with photocell beams. The number of beam breaks was recorded over 1 hour.

253 ***Ex vivo* electrophysiological recordings**

254 We performed whole-cell patch-clamp recordings of neurons from the layer II/III of the ACC.
255 Local electrical stimulation was delivered by a bipolar stimulation electrode placed in layer V/VI
256 of the ACC. For these experiments, mice were killed by decapitation and the brain was removed,
257 then immediately immersed in cold (0-4°C) sucrose-based artificial cerebrospinal fluid
258 containing (in mM): 2 kynurenic acid, 248 sucrose, 11 glucose, 26 $NaHCO_3$, 2 KCl, 1.25
259 KH_2PO_4, 2 $CaCl_2$ and 1.3 $MgSO_4$ (bubbled with 95% O_2 and 5% CO_2). Transverse slices (300
260 µm thick) were cut with a vibratome (VT1000S, Leica, Nussloch, Germany). Slices were
261 maintained at room temperature in a chamber filled with artificial cerebrospinal fluid containing
262 (in mM): 126 NaCl, 26 $NaHCO_3$, 2.5 KCl, 1.25 NaH_2PO_4, 2 $CaCl_2$, 2 $MgCl_2$ and 10 glucose
263 (bubbled with 95% O_2 and 5% CO_2; pH 7.3; 310 mOsm measured). Slices were transferred to a
264 recording chamber and continuously superfused with artificial cerebrospinal fluid saturated with
265 95% O_2 and 5% CO_2. Pyramidal ACC neurons were recorded in the whole-cell patch
266 configuration. Patch pipettes were pulled from borosilicate glass capillaries (Harvard Apparatus,
267 Edenbridge, UK) using a P-1000 puller (Sutter Instruments, Novato, CA, USA). For optogenetic
268 experiments performed in AAV5-CaMKIIa-eArchT3.0-EYFP injected animals, pipettes were
269 filled with a solution containing the following (in mM): 145 KCl, 10 HEPES and 2 $MgCl_2$. For
270 mEPSCs recordings, pipettes were filled with a solution containing the following (in mM): 75
271 Cs_2SO_4, 10 CsCl, 10 HEPES and 2 $MgCl_2$. The pH of intrapipette solutions was adjusted to 7.3
272 with KOH, and osmolarity to 310 mOsm with sucrose. With this solution, the patch pipettes had
273 an open tip resistance from 3.5 to 4.5 MΩ. Recordings were performed in the presence of CNQX
274 (10 µM) and bicuculline (10 µM) for optogenetic experiments, while mEPSCs were recorded
275 with tetrodotoxin (TTX, 0.5 µM) in the recording solution. For optogenetic experiments, the
276 ACC was illuminated with the same system used for the *in vivo* experiments (see below)

277 triggered with WinWCP 4.3.5, the optic fiber being localized in the recording chamber at 3 mm
278 from the recorded neuron. In voltage-clamp mode, the holding potential was fixed at -60 mV, and
279 in current-clamp mode at a holding current allowing maintaining the resting neuron at ca. -60
280 mV. Recordings were acquired with WinWCP 4.3.5 (courtesy of Dr. J. Dempster, University of
281 Strathclyde, Glasgow, Scotland). All recordings were performed at 34°C.
282
283 ***In vivo* electrophysiological recordings**
284 Animals were anesthetized in an induction box with a 2% isoflurane/air mixture (Vetflurane,
285 Virbac) and then placed in a Kopf stereotaxic frame (KOPF 1730) equipped with a tight nose
286 mask to continuously deliver the anesthesia.
287 A 1 x 1.4 mm cranial window was prepared directly anterior to the bregma, ranging -0.7 to
288 0.7 mm lateral from the midline. The dura was opened to lower the glass electrode into the brain.
289 Recordings of spontaneous activity were performed using sharp electrodes pulled from
290 borosilicate micropipettes (1.2 mm outer and 0.69 mm inner diameters, Harvard Apparatus, 30-
291 0044), with a Narashige pipette puller (tip diameter < 1 µm, resistance ±25 MΩ). The glass
292 electrodes were filled with 0.5 M potassium acetate solution. The signal from the electrode was
293 recorded by a silver wire, amplified using an operational amplifier (Neurodata IR-183A, Cygnus
294 Technology inc.; gain x 10), and then amplified further and filtered using a differential amplifier
295 (Model 440, Brownlee Precision; gain x 100; band pass filter 0.1-10 kHz). The signal was then
296 digitized with a CED digitizer (sampling rate: 20 kHz) and recorded with Spike2 software
297 (Version 7.12b, Cambridge Electronic Design, Cambridge, UK). Raw data files were exported
298 into Matlab and analyzed with custom-made Matlab scripts which are available in a bitbucket
299 repository (Sellmeijer, 2016).

During the recording procedure, isoflurane anesthesia was lowered to 0.5-0.75% and was monitored by regular paw pinching. The glass pipette was slowly lowered using a Scientifica one dimensional micromanipulator and recordings were made between 0.2 and 1.0 mm anterior to the bregma ranging from -0.5 to +0.5 mm from the midline, which corresponds to layers II/III of the cortex. Neurons were recorded from the brain surface until 1500 µm deep. Once stable cell activity was detected, a 5 minute segment of spontaneous activity was recorded. Recording sites were marked by iontophoretically injecting a 4% Pontamine Sky blue dye (Sigma) in 0.5 M sodium-acetate solution (Sigma). At the end of the recording, the mice were perfused, the brain was collected, and 40 µm sections were cut on a cryostat. The position of recorded cells was registered using the microdrive reference point with respect to the Pontamine Sky blue dye deposit.

Firing rate and bursting activity were calculated. Bursting activity, defined as 3 or more spikes within a 50 msec time window, was analyzed by calculating the total number of bursting events within a 90 second data segment. Neurons in which more than 20% of action potentials occurred in a bursting event were considered bursting neurons. The average number of spikes within a bursting event was also calculated.

Experimental design and statistical analysis

Before starting experiments, based on our previous behavioral studies, we estimated the sample size by using power analysis. All behavioral tests, *in vivo* electrophysiological recordings, and experiments using optogenetic approach were replicated several times. For each group, the mechanical sensitivity and anxiodepressive-like behaviors were analyzed before recordings and optogenetic manipulation. The number of animals per group is indicated in each behavioral graph; and both the number of recorded cells and of animals per group is indicated in each

electrophysiology graph. Data are expressed as mean ± SEM. When data were not normally distributed, the Kruskal-Wallis test was performed followed by Mann-Whitney U post-hoc tests to compare the means. When data were normally distributed, groups were compared with ANOVA multiple group comparisons followed by Duncan post-hoc analysis, or with the student *t*-test. For the von Frey results, we used a multifactorial ANOVA, considering paws (ipsilateral vs contralateral) and time points as 2 levels of dependent data, and surgery (sham vs. cuff) as independent groups. Significance level was set to $p<0.05$. Statistical analyses were performed with Matlab 2014a (Matworks inc.) and STATISTICA 7.1 (Statsoft, Tulsa, Oklahoma).

Results

Long-term characterization of different symptoms of neuropathic pain

It has been previously shown that the anxiodepressive-like consequences of neuropathic pain evolve over time (Suzuki et al., 2007; Goncalves et al., 2008; Yalcin et al., 2011). Indeed, whereas mechanical hypersensitivity is immediately present following nerve injury in the cuff model, mice develop anxiety-related behaviors 3-4 weeks (W) later, while depression-related behaviors are observed after 6-8 W (Yalcin et al., 2011). On the longer term, cuff-implanted animals recover spontaneously from mechanical hypersensitivity (example from one batch of mice: $F_{(13,260)}=5.54$, $p=6.9*10^{-9}$, cuff<sham: 1st $p=2.7*10^{-6}$, 3rd $p=8.8*10^{-7}$, 5th $p=1*10^{-6}$, 7th $p=1.8*10^{-6}$ and 9th W $p=1.5*10^{-6}$; **Figure 1**). Depending on the considered batch of animals, this recovery happened between the 11th and 14th W post-operation (PO). However, it is to be noted that all mice displayed mechanical hypersensitivity up to the 10th W PO, and that no mice was hypersensitive at 15 W PO. This recovery from mechanical hypersensitivity raises the question of whether the aversiveness of ongoing pain and/or the anxiodepressive-like consequences of chronic pain also disappear or remain present.

As reported previously (Yalcin et al., 2011), the nerve-injured animals did not show anxiodepressive-like behaviors yet at 2 W PO (dark-light test, **Figure 2A**; novelty suppressed feeding (NSF) test, **Figure 2C**) or at 3 W PO (splash test, **Figure 2B**), even though mechanical hypersensitivity was already present (VF: p=0.01 **(Figure 2A)**; p=0.0001 **(Figure 2B)**; p=0.001 **(Figure 2C)**). In the dark-light test, nerve-injured animals displayed increased anxiety-like behavior at 8 W PO, as shown by the reduced time spent in the lit compartment ($p=6.17*10^{-4}$, **Figure 2A**). This behavior disappeared at 11 and 15 W PO, coinciding with the recovery from mechanical hypersensitivity in the same animals (see **Figure 1**). In contrast, in the splash test, decreased grooming behavior was present at 9 W PO (p=0.01), but also at 12 W (p=0.003) and 14 W PO (p=0.0011) (**Figure 2B**) despite that mechanical hypersensitivity was no longer present in these sets of animals at these last 2 time-points. The deficit in grooming behavior, however, disappeared at 16 W PO (**Figure 2B**). Recovery was even more delayed in the novelty suppressed feeding (NSF) test, for which an increased latency to feed was present at 8 ($p=3.3*10^{-4}$), 11 (p=0.0437) and 16 W PO (p=0.0016) (with no mechanical hypersensitivity at these last 2 time-points), with recovery at 18 and 21 W PO (**Figure 2C**). The presence of depressive-like behavior as assessed using the forced swimming test (FST) was also long-lasting. Indeed, nerve-injured mice spent more time immobile at 7 ($p=4.33*10^{-5}$), 14 (p=0.0043) and 17 W PO (p=0.0023) (with no mechanical hypersensitivity at these last 2 time-points) (**Figure 2D**), and returned back to sham level only at 18 and 21 W PO (**Figure 2D**). Each von Frey result obtained the same week as the anxiodepressive behavioral tests is presented nearby the anxiodepressive behavioral graph (Figure 2A-D).

Since the time course of recovery from mechanical hypersensitivity could slightly differ between batches of experiments, the results are presented according to 4 representative Time Points (TP) for the rest of this study. TP1 corresponds to animals displaying mechanical

hypersensitivity but not yet anxiodepressive-like consequences, TP2 corresponds to animals displaying both mechanical hypersensitivity and anxiodepressive-like consequences, TP3 corresponds to animals which recovered from mechanical hypersensitivity but still displayed depressive-like consequences, and TP4 corresponds to animals which recovered from both mechanical hypersensitivity and anxiodepressive-like consequences.

As a control for behavioral tests, we checked the locomotor activity of animals over 1hr at different time points and confirmed our previous reports (Barthas et al., 2015; Barthas et al., 2017) by showing that locomotor activity was not significantly affected in cuff implanted-animals at the representative TP1, 2 and 3 (**Figure 2E**).

We then tested the aversiveness of ongoing pain by using a conditioned place preference (CPP) test. Clonidine was delivered intrathecally at lumbar level, which inhibits ascending inputs and leads to pain relief. Nerve-injured animals displayed a significant preference for the compartment associated with clonidine analgesia at TP2 ($F_{(1,9)}$=5.36, p=0.04, cuff saline vs cuff clonidine p=0.017) **Figure 3A**, but also at TP3 ($F_{(1,12)}$=5.219, p=0.04, cuff saline vs cuff clonidine p=0.03, **Figure 3B**), despite the absence of mechanical hypersensitivity at this time-point. Interestingly, this preference was no longer present at TP4 ($F_{(1,11)}$=0.36, p=0.55, **Figure 3C**), suggesting a recovery from ongoing pain. See also the **Figure 3A, B** and **C** for the state of mechanical hypersensitivity (TP2, $p=6.2*10^{-5}$; TP3, p=0.34; TP 4, p=0.58) and of anxiodepressive-like consequences (TP2, p=0.0028; TP3, p=0.0014; TP4, p=0.83) in the same mice.

Together, these data show that ongoing pain and the depressive-like consequences of neuropathic pain can persist for weeks after the recovery from mechanical hypersensitivity.

ACC hyperactivity coincides with anxiodepressive-like consequences of neuropathic pain

To understand whether the spontaneous activity of the ACC is affected along the time-dependent evolution of neuropathic pain symptoms, we performed *in vivo* single unit electrophysiological recording (**Figure 4A**) at 4 different TPs (**Figure 4B**). ACC neurons from nerve-injured animals had a significantly higher *in vivo* spontaneous firing rate at TP2 ($p=3.52*10^{-7}$) and TP3 ($p=0.0022$; **Figures 4C, D**), which was associated with an increase in bursting activity (TP2: $p=5.50*10^{-5}$, TP3: $p=0.017$; **Figure 4E**), in the number of action potentials per burst ($p=3.42*10^{-5}$, **Figure 4F**) and in the number of bursting cells ($p=0.034$, **Figure 4F**) in nerve-injured animals at TP2. In the absence of anxiodepressive-like behaviors, i.e. at TP1 (before affective symptoms developed) and at TP4 (after affective symptoms recovered), the firing rate and bursting activity remained similar between sham and nerve-injured animals (**Figures 4D,E**). No significant lateralization effect was measured for firing rate and bursting activity in cuff implanted animals (data not shown).

Enhancement of excitatory synaptic transmission in the ACC coincides with anxiodepressive-like consequences of neuropathic pain

To assess the impact of neuropathic pain on synaptic transmission of pyramidal neurons, we recorded both paired-pulse ratio and miniature synaptic currents at TP2, when nerve-injured animals displayed depressive-like behavior. There was a significant reduction in the paired-pulse ratio of electrically-evoked EPSCs, which provides support for presynaptic changes in nerve-injured mice ($F_{(1,120)}=30.8$, $p<0.001$, **Figure 5A**). Both the amplitude and frequency of miniature excitatory postsynaptic currents (mEPSCs) (amplitude: sham mice 7.8 ± 0.4 pA, cuff mice 9.8 ± 0.6 pA, $p<0.05$; frequency: sham mice 1.2 ± 0.1 Hz, cuff mice 2.2 ± 0.2 Hz, $p<0.01$, **Figure 5B**) were significantly increased in nerve-injured mice, indicating that the facilitation of excitatory synaptic transmission onto pyramidal ACC neurons involved presynaptic and postsynaptic

changes. Interestingly, both the slopes of the AMPAR mediated input-output curve ($F_{(1,97)}$=17.1, $p<0.001$, **Figure 5C**, left) and NMDAR mediated input-output curve ($F_{(1,55)}$=7.7, $p<0.01$, **Figure 5D**, left) were shifted to the left in nerve-injured mice, suggesting that an upregulation of AMPA and NMDA receptors could contribute to excitatory facilitation. We then tested the AMPAR and NMDAR mediated I-V relationship and found that there was no difference in the AMPAR mediated I-V between sham and nerve-injured mice ($F_{(1,108)}$=2.0, p=0.15, **Figure 5C**, right). However, the NMDAR mediated I-V curve differed between groups ($F_{(1,153)}$=61.3, $p<0.01$, **Figure 5D**). When the same experiments were performed at TP3, which corresponds to animals still displaying depressive-like behaviors after recovery from mechanical hypersensitivity, we observed that the mEPSC frequency was still increased ($F_{(1,19)}$=8.974; p=0.008 **Figure 6**), but not the paired-pulse ratio of evoked EPSCs. This finding indicates that the spontaneous release of glutamate was still enhanced in the ACC after the recovery from mechanical hypersensitivity. Neither the AMPAR nor the NMDAR mediated input and output curves were altered. Interestingly, the NMDAR I-V curve remained different in the cuff group ($F_{(1,108)}$=15.54; p=0.001, **Figure 6**).

Inhibition of the ACC relieves the emotional consequences of neuropathic pain

Based on our results demonstrating ACC hyperactivity in mice displaying anxiodepressive-like behaviors, we studied whether optogenetic inhibition of the ACC may counteract these consequences.

The delivery of AAV5-CaMKIIa-eArchT3.0-EYFP resulted in reliable virus transfection in the ACC, which was confirmed by EYFP fluorescence (**Figure 7A**). To characterize the effect of green laser light illumination on transfected ACC neurons, we performed *ex vivo* electrophysiological recordings. Patch-clamp recordings showed that illumination with green

light reliably inhibited spontaneous action potential firing in the current-clamp mode, and induced an outward current in the voltage clamp mode (**Figure 7B**).

In vivo, mechanical hypersensitivity was not affected by the ACC inhibition at either TP2 ($F_{(1,26)}$=60.29, p=0.3*10^{-8}, cuff right < sham right, p=0.0001) or TP3 ($F_{(1,20)}$=0.0032, p=0.95,) (**Figure 7C**). However, inhibition of the targeted ACC neurons induced a place preference in nerve-injured animals at both time-points, i.e. when mechanical hypersensitivity was still present (TP2, $F_{(1,18)}$=5.42, p=0.031, cuff stimulated (light on) vs cuff control p=0.006) (**Figure 7D**) or after it recovered (TP3, $F_{(1,8)}$=8.66, p=0.018, cuff stimulated (light on) vs cuff control p=0.039, **Figure 7D**), without having any effect in sham animals. These findings indicate that the inhibition of the CaMKIIa ACC neurons relieved the aversiveness of ongoing pain in nerve-injured mice.

Finally, we showed that optogenetic inhibition of the ACC also suppressed the anxiodepressive-like behaviors in nerve-injured animals, as observed by a normalization of grooming behavior in the splash test (**Figure 7E**) at both TP2 (p=0.0033, cuff no light versus cuff light on) and TP3 (p=0.03, cuff no light versus cuff light on), and of the feeding latency in the NSF test at TP2 (p=0.0013) (**Figure 7F**). “No-light delivered” nerve-injured animals, however, still displayed characteristic chronic pain induced-behaviors (sham no-light vs cuff no-light grooming duration: p=0.03, TP2; p=0.01, TP3; **Figure 7E**; sham no-light vs cuff no-light latency to feed: p=0.015, TP2; p=0.015, TP3; **Figure 7F**). Altogether, our results show that a selective inhibition of ACC excitatory neurons is sufficient to alleviate the long-lasting consequences of neuropathic pain.

Discussion

We show here that different symptoms of neuropathic pain, including mechanical hypersensitivity, aversiveness of ongoing pain, and anxiodepressive-like consequences, display different time courses following nerve injury. The *in vivo* electrophysiological recordings showed an ACC hyperactivity coinciding with the time window of pain aversiveness and of anxiodepressive-like behaviors. *Ex vivo* patch-clamp recordings further supported ACC hyperactivity, as shown by increased excitatory postsynaptic transmission and increased contribution of NMDA receptors. Finally, our results show that optogenetic inhibition of the ACC can alleviate the aversiveness and anxiodepressive-like consequences of neuropathic pain.

A growing number of preclinical studies shows that the anxiodepressive-like consequences of chronic pain evolve over time (Yalcin et al., 2011; Alba-Delgado et al., 2013), raising the question of whether the various symptoms of neuropathic pain are inter-dependent or whether they develop separately. With the model and species used in this study, animals develop mechanical hypersensitivity immediately after nerve injury, and spontaneously recover around 3 months later, which allows studying the behavioral consequences of neuropathic pain in the presence and absence of mechanical hypersensitivity. Patients with chronic pain also experience ongoing pain, which is rarely evaluated in preclinical studies. In animals, this symptom can be unmasked by alleviating the pain-related tonic aversive state in a CPP procedure (King et al., 2009; Barthas et al., 2015). For instance, lidocaine injected into the rostral ventromedial medulla, the brain area mediating descending modulation of pain (Wang et al., 2013), or spinal injection of clonidine (King et al., 2009; Barthas et al., 2015), induce place preference only in nerve-injured animals. In the present study, we also detected the presence of ongoing pain at TP3, i.e. when mechanical hypersensitivity is no longer present, a finding that represents, to our knowledge, the first evidence in an animal model for a naturally-occurring temporal dichotomy between evoked

and ongoing pain. The hypersensitivity and ongoing pain that follow nerve injury have been proposed to share some mechanistic features. Indeed, both may imply an upregulation of voltage-gated Nav1.8 channels in primary afferent neurons (Yang et al., 2014), an alteration of descending pathways (Wang et al., 2013) and of spinal NK-1 positive ascending projections (King et al., 2011). Studies also pointed out that they can be distinguished mechanistically as well as neuroanatomically. An ACC lesion can block the aversiveness of ongoing pain in both neuropathic (Qu et al., 2011; Barthas et al., 2015) and inflammatory pain models without affecting mechanical hypersensitivity (Johansen et al., 2001; Chen et al., 2014; Barthas et al., 2015), whereas lesioning the posterior insular cortex can suppress the maintenance of mechanical hypersensitivity (Benison et al., 2011; Barthas et al., 2015) without affecting ongoing pain (Barthas et al., 2015). In addition, large-diameter fibers of the dorsal column were proposed to mediate mechanical hypersensitivity but not ongoing pain (King et al., 2011). This dichotomy should, thus, be taken into consideration for drug development, since mechanical hypersensitivity, rather than ongoing pain, is presently used for target validation. As it is more often ongoing pain that leads patients to seek treatment, this may in part explain why the development of new treatments has not always provided translational satisfaction.

While mechanical hypersensitivity is no longer present around 3 months PO, we still observed depressive-like behaviors. Previously, it has been reported in mice that anxiodepressive-like behaviors can persist at least 10 days after normalization of mechanical sensitivity following cuff removal (Dimitrov et al., 2014). Our results confirm and further extend this hypersensitivity/affective dichotomy by showing that aversiveness and depressive-like symptoms persist at least 3 to 6W after cessation of hypersensitivity. We also show that recovery from anxiety-like behaviors is faster, happening almost 6W before the loss of depressive-like consequences, and that it coincides with the disappearance of mechanical hypersensitivity. It is

important to consider that the detailed time-courses for the various behavioral consequences of neuropathic pain likely depend on the considered species, strain and pain model or etiology, as already suggested by published reports (Yalcin et al., 2014a).

The prolonged emotional consequences point out the presence of long-term plastic changes in the brain, secondary to a peripheral nerve injury. One of the cortical regions where such morphological (Blom et al., 2014; Yalcin et al., 2014b), molecular (Barthas et al., 2017) and functional plasticity (Li et al., 2010; Koga et al., 2015) has been reported is the ACC. Our *in vivo* single unit extracellular recordings showed an increased firing rate and bursting activity in the ACC at TP2 and 3, coinciding with aversive and depressive-like behaviors. Interestingly, the ACC hyperactivity persists even after anxiety-like behaviors disappeared, suggesting that this hyperactivity may be important but not sufficient for the anxiety-like behavior. In humans, fMRI studies have shown that the ventral part of the ACC, which is involved in emotional processing (Kanske and Kotz, 2012), is hyperactive in depressed patients (Mayberg et al., 1999; Yoshimura et al., 2010), and that activity patterns in ACC subregions correlated with symptom clusters such as sadness and depressed mood (Mayberg et al., 1999). This possible role of ACC is further supported by animal studies showing increased cingulate cortex activity accompanying depressive-like behaviors in a social-defeat paradigm, as evidenced by c-Fos overexpression (Yu et al., 2011), and in the present model of nerve-injured mice, as evidenced by enhanced phosphorylation of the transcription factors cyclic adenosine monophosphate (cAMP) response element binding protein (CREB) and activating transcription factor (ATF) as well as by enhanced cAMP responsive element-driven transcriptional activity and by c-Fos expression (Barthas et al., 2017). While it has been hypothesized that the abnormal ACC activity in depression can be associated with changes in GABA interneurons, since levels of somatostatin (Seney et al., 2015) and parvalbumin (Tripp et al., 2012) are low in patients with major depressive disorders

(Northoff and Sibille, 2014), 80% of ACC neurons are pyramidal ones, and the optogenetic inhibition of CaMKII-expressing ACC neurons blocks the anxiodepressive-like behaviors induced by chronic pain. Moreover, we previously showed that optogenetic activation of pyramidal neurons was sufficient to drive anxiodepressive-like behaviors in naive mice (Barthas et al., 2015; Barthas et al., 2017). While these data indirectly support an implication of pyramidal neurons in ACC hyperactivity, the shape of spikes did not allow differentiating neuronal subtypes responsible for the *in vivo* increased firing activity. However, our *ex vivo* recordings further show that ACC might also be linked to a long-term increase in excitatory synaptic transmission. This hyperactivity could be supported by long-term alterations in functional connections onto pyramidal neurons, which may be initiated at an early stage of the neuropathy (Koga et al., 2015) and participate in the long lasting presence of affective symptoms. Here, all the recordings were performed in layers II-III since these neurons receive both sensory inputs from the thalamus and inputs from the basal forebrain, including amygdala ones; and we previously reported that synapses in layers II-III undergo plastic changes after LTP induction or peripheral nerve injury (Koga et al., 2015; Song et al., 2017).

To leap from correlative analyses to a causal link between ACC hyperactivity and the behavioral outputs of neuropathic pain, we performed optogenetic inhibition of the ACC. We showed that the inhibition of the ACC suppressed the aversiveness of ongoing pain and the depressive-like consequences of neuropathic pain without affecting mechanical hypersensitivity at TP2 and TP3. These results further reinforce the links between pain aversiveness and depressive-like consequences on the one hand, and between ACC hyperactivity and these emotional aspects of chronic pain on the other. Together with our recent data showing that optogenetic recapitulation of the ACC hyperactivity by using channelrhodopsin 2 (Barthas et al., 2015; Barthas et al., 2017) is sufficient to drive anxiodepressive-like behaviors in naïve animals,

the present data with archaerhodopsin further support the hypothesis that ACC hyperactivity is critical to anxiodepressive-like behaviors. Conversely, it has been shown that inhibiting ACC pyramidal neurons (Kang et al., 2015) or activating inhibitory neurons (Gu et al., 2015) can acutely reduce the hypersensitivity induced by Freund's complete adjuvant or formalin respectively, as also observed with pharmacological manipulation at early stages of neuropathic pain (Li et al., 2010). It suggests that ACC manipulation might also affect nociceptive hypersensitivity in given conditions.

In conclusion, our results emphasize that anxiodepressive-like consequences of chronic pain can experimentally be segregated from mechanical hypersensitivity in a time dependent manner, whereas they follow the same time course as the aversiveness of ongoing pain. This time dependency between symptoms should be taken into consideration to improve the translational features of preclinical models, and for preclinical target validation of relevant potential therapies. The fact that the emotional consequences of chronic pain are driven by ACC hyperactivity further highlights the ACC and its circuitry as critical neuroanatomical substrates to further explore mood disorder mechanisms. Such circuitry analysis requires a precise knowledge of the ACC connectome, which was recently detailed in mice (Fillinger et al., 2017b, a). Together with present behavioral characterization and electrophysiological data, these information should now allow reaching circuit-level of analysis, including concerning the question of critical input(s) required to induce ACC hyperactivity, and of whether maintaining ACC hyperactivity requires or not input(s) hyperactivity.

585 **References**

586 Alba-Delgado C, Llorca-Torralba M, Horrillo I, Ortega JE, Mico JA, Sanchez-Blazquez P, Meana JJ,
587 Berrocoso E (2013) Chronic pain leads to concomitant noradrenergic impairment and mood
588 disorders. Biol Psychiatry 73:54-62.
589 Barrot M (2012) Tests and models of nociception and pain in rodents. Neuroscience 211:39-50.
590 Barthas F, Sellmeijer J, Hugel S, Waltisperger E, Barrot M, Yalcin I (2015) The anterior cingulate cortex is a
591 critical hub for pain-induced depression. Biol Psychiatry 77:236-245.
592 Barthas F, Humo M, Gilsbach R, Waltisperger E, Karatas M, Leman S, Hein L, Belzung C, Boutillier AL,
593 Barrot M, Yalcin I (2017) Cingulate Overexpression of Mitogen-Activated Protein Kinase
594 Phosphatase-1 as a Key Factor for Depression. Biol Psychiatry 82:370-379.
595 Benbouzid M, Choucair-Jaafar N, Yalcin I, Waltisperger E, Muller A, Freund-Mercier MJ, Barrot M (2008)
596 Chronic, but not acute, tricyclic antidepressant treatment alleviates neuropathic allodynia after
597 sciatic nerve cuffing in mice. Eur J Pain 12:1008-1017.
598 Benison AM, Chumachenko S, Harrison JA, Maier SF, Falci SP, Watkins LR, Barth DS (2011) Caudal
599 granular insular cortex is sufficient and necessary for the long-term maintenance of allodynic
600 behavior in the rat attributable to mononeuropathy. J Neurosci 31:6317-6328.
601 Bliss TV, Collingridge GL, Kaang BK, Zhuo M (2016) Synaptic plasticity in the anterior cingulate cortex in
602 acute and chronic pain. Nat Rev Neurosci 17:485-496.
603 Blom SM, Pfister JP, Santello M, Senn W, Nevian T (2014) Nerve injury-induced neuropathic pain causes
604 disinhibition of the anterior cingulate cortex. J Neurosci 34:5754-5764.
605 Chen T, Koga K, Descalzi G, Qiu S, Wang J, Zhang LS, Zhang ZJ, He XB, Qin X, Xu FQ, Hu J, Wei F, Huganir
606 RL, Li YQ, Zhuo M (2014) Postsynaptic potentiation of corticospinal projecting neurons in the
607 anterior cingulate cortex after nerve injury. Mol Pain 10:33.
608 Cordeiro Matos S, Zhang Z, Seguela P (2015) Peripheral Neuropathy Induces HCN Channel Dysfunction in
609 Pyramidal Neurons of the Medial Prefrontal Cortex. J Neurosci 35:13244-13256.
610 Dimitrov EL, Tsuda MC, Cameron HA, Usdin TB (2014) Anxiety- and depression-like behavior and
611 impaired neurogenesis evoked by peripheral neuropathy persist following resolution of
612 prolonged tactile hypersensitivity. J Neurosci 34:12304-12312.
613 Drevets WC, Bogers W, Raichle ME (2002) Functional anatomical correlates of antidepressant drug
614 treatment assessed using PET measures of regional glucose metabolism. Eur
615 Neuropsychopharmacol 12:527-544.
616 Fillinger C, Yalcin I, Barrot M, Veinante P (2017a) Efferents of anterior cingulate areas 24a and 24b and
617 midcingulate areas 24a' and 24b' in the mouse. Brain Struct Funct.
618 Fillinger C, Yalcin I, Barrot M, Veinante P (2017b) Afferents to anterior cingulate areas 24a and 24b and
619 midcingulate areas 24a' and 24b' in the mouse. Brain Struct Funct 222:1509-1532.
620 Goncalves L, Silva R, Pinto-Ribeiro F, Pego JM, Bessa JM, Pertovaara A, Sousa N, Almeida A (2008)
621 Neuropathic pain is associated with depressive behaviour and induces neuroplasticity in the
622 amygdala of the rat. Exp Neurol 213:48-56.
623 Gu L, Uhelski ML, Anand S, Romero-Ortega M, Kim YT, Fuchs PN, Mohanty SK (2015) Pain inhibition by
624 optogenetic activation of specific anterior cingulate cortical neurons. PLoS One 10:e0117746.
625 Johansen JP, Fields HL, Manning BH (2001) The affective component of pain in rodents: direct evidence
626 for a contribution of the anterior cingulate cortex. Proc Natl Acad Sci U S A 98:8077-8082.
627 Kang SJ, Kwak C, Lee J, Sim SE, Shim J, Choi T, Collingridge GL, Zhuo M, Kaang BK (2015) Bidirectional
628 modulation of hyperalgesia via the specific control of excitatory and inhibitory neuronal activity
629 in the ACC. Mol Brain 8:81.
630 Kanske P, Kotz SA (2012) Effortful control, depression, and anxiety correlate with the influence of
631 emotion on executive attentional control. Biol Psychol 91:88-95.

632 King T, Vera-Portocarrero L, Gutierrez T, Vanderah TW, Dussor G, Lai J, Fields HL, Porreca F (2009)
633 Unmasking the tonic-aversive state in neuropathic pain. Nat Neurosci 12:1364-1366.
634 King T, Qu C, Okun A, Mercado R, Ren J, Brion T, Lai J, Porreca F (2011) Contribution of afferent pathways
635 to nerve injury-induced spontaneous pain and evoked hypersensitivity. Pain 152:1997-2005.
636 Koga K, Descalzi G, Chen T, Ko HG, Lu J, Li S, Son J, Kim T, Kwak C, Huganir RL, Zhao MG, Kaang BK,
637 Collingridge GL, Zhuo M (2015) Coexistence of two forms of LTP in ACC provides a synaptic
638 mechanism for the interactions between anxiety and chronic pain. Neuron 85:377-389.
639 Li XY, Ko HG, Chen T, Descalzi G, Koga K, Wang H, Kim SS, Shang Y, Kwak C, Park SW, Shim J, Lee K,
640 Collingridge GL, Kaang BK, Zhuo M (2010) Alleviating neuropathic pain hypersensitivity by
641 inhibiting PKMzeta in the anterior cingulate cortex. Science 330:1400-1404.
642 Mayberg HS, Liotti M, Brannan SK, McGinnis S, Mahurin RK, Jerabek PA, Silva JA, Tekell JL, Martin CC,
643 Lancaster JL, Fox PT (1999) Reciprocal limbic-cortical function and negative mood: converging
644 PET findings in depression and normal sadness. Am J Psychiatry 156:675-682.
645 Narita M, Kaneko C, Miyoshi K, Nagumo Y, Kuzumaki N, Nakajima M, Nanjo K, Matsuzawa K, Yamazaki M,
646 Suzuki T (2006) Chronic pain induces anxiety with concomitant changes in opioidergic function in
647 the amygdala. Neuropsychopharmacology 31:739-750.
648 Northoff G, Sibille E (2014) Why are cortical GABA neurons relevant to internal focus in
649 depression[quest] A cross-level model linking cellular, biochemical and neural network findings.
650 Mol Psychiatry 19:966-977.
651 Peyron R, Garcia-Larrea L, Gregoire MC, Convers P, Richard A, Lavenne F, Barral FG, Mauguiere F, Michel
652 D, Laurent B (2000) Parietal and cingulate processes in central pain. A combined positron
653 emission tomography (PET) and functional magnetic resonance imaging (fMRI) study of an
654 unusual case. Pain 84:77-87.
655 Porsolt RD, Le Pichon M, Jalfre M (1977) Depression: a new animal model sensitive to antidepressant
656 treatments. Nature 266:730-732.
657 Qu C, King T, Okun A, Lai J, Fields HL, Porreca F (2011) Lesion of the rostral anterior cingulate cortex
658 eliminates the aversiveness of spontaneous neuropathic pain following partial or complete
659 axotomy. Pain 152:1641-1648.
660 Radat F, Margot-Duclot A, Attal N (2013) Psychiatric co-morbidities in patients with chronic peripheral
661 neuropathic pain: a multicentre cohort study. Eur J Pain 17:1547-1557.
662 Seney ML, Tripp A, McCune S, A. Lewis D, Sibille E (2015) Laminar and cellular analyses of reduced
663 somatostatin gene expression in the subgenual anterior cingulate cortex in major depression.
664 Neurobiology of Disease 73:213-219.
665 Shackman AJ, Salomons TV, Slagter HA, Fox AS, Winter JJ, Davidson RJ (2011) The integration of negative
666 affect, pain and cognitive control in the cingulate cortex. Nat Rev Neurosci 12:154-167.
667 Song Q, Zheng HW, Li XH, Huganir RL, Kuner T, Zhuo M, Chen T (2017) Selective Phosphorylation of
668 AMPA Receptor Contributes to the Network of Long-Term Potentiation in the Anterior Cingulate
669 Cortex. J Neurosci 37:8534-8548.
670 Surget A, Wang Y, Leman S, Ibarguen-Vargas Y, Edgar N, Griebel G, Belzung C, Sibille E (2009)
671 Corticolimbic transcriptome changes are state-dependent and region-specific in a rodent model
672 of depression and of antidepressant reversal. Neuropsychopharmacology 34:1363-1380.
673 Suzuki T, Amata M, Sakaue G, Nishimura S, Inoue T, Shibata M, Mashimo T (2007) Experimental
674 neuropathy in mice is associated with delayed behavioral changes related to anxiety and
675 depression. Anesth Analg 104:1570-1577, table of contents.
676 Tang J, Ko S, Ding H-K, Qiu C-S, Calejesan AA, Zhuo M (2005) Pavlovian fear memory induced by
677 activation in the anterior cingulate cortex. Molecular pain 1:6

678 Tripp A, Oh H, Guilloux JP, Martinowich K, Lewis DA, Sibille E (2012) Brain-derived neurotrophic factor
679 signaling and subgenual anterior cingulate cortex dysfunction in major depressive disorder. Am J
680 Psychiatry 169:1194-1202.
681 Vogt MA, Mallien AS, Pfeiffer N, Inta I, Gass P, Inta D (2016) Minocycline does not evoke anxiolytic and
682 antidepressant-like effects in C57BL/6 mice. Behav Brain Res 301:96-101.
683 Wang R, King T, De Felice M, Guo W, Ossipov MH, Porreca F (2013) Descending facilitation maintains
684 long-term spontaneous neuropathic pain. J Pain 14:845-853.
685 Xu H, Wu LJ, Wang H, Zhang X, Vadakkan KI, Kim SS, Steenland HW, Zhuo M (2008) Presynaptic and
686 postsynaptic amplifications of neuropathic pain in the anterior cingulate cortex. J Neurosci
687 28:7445-7453.
688 Yalcin I, Barthas F, Barrot M (2014a) Emotional consequences of neuropathic pain: insight from
689 preclinical studies. Neurosci Biobehav Rev 47:154-164.
690 Yalcin I, Bohren Y, Waltisperger E, Sage-Ciocca D, Yin JC, Freund-Mercier MJ, Barrot M (2011) A time-
691 dependent history of mood disorders in a murine model of neuropathic pain. Biol Psychiatry
692 70:946-953.
693 Yalcin I, Megat S, Barthas F, Waltisperger E, Kremer M, Salvat E, Barrot M (2014b) The sciatic nerve
694 cuffing model of neuropathic pain in mice. J Vis Exp.
695 Yang Q, Wu Z, Hadden JK, Odem MA, Zuo Y, Crook RJ, Frost JA, Walters ET (2014) Persistent pain after
696 spinal cord injury is maintained by primary afferent activity. J Neurosci 34:10765-10769.
697 Yoshimura S, Okamoto Y, Onoda K, Matsunaga M, Ueda K, Suzuki S, Shigetoyamawaki (2010) Rostral
698 anterior cingulate cortex activity mediates the relationship between the depressive symptoms
699 and the medial prefrontal cortex activity. J Affect Disord 122:76-85.
700 Yu T, Guo M, Garza J, Rendon S, Sun XL, Zhang W, Lu XY (2011) Cognitive and neural correlates of
701 depression-like behaviour in socially defeated mice: an animal model of depression with
702 cognitive dysfunction. Int J Neuropsychopharmacol 14:303-317.

703 **Figure Legends**

704 **Figure 1. Nerve injury induces mechanical hypersensitivity.** In C57BL/6J mice, unilateral
705 sciatic nerve compression induces an ipsilateral long-lasting mechanical hypersensitivity which
706 lasts around 11 weeks. After this period, mechanical thresholds return back to sham levels
707 spontaneously. Sham n=24; Cuff n=24 Data are expressed as mean ± SEM. *** $p< 0.001$. PWT:
708 Paw withdrawal threshold.

709 **Figure 2. Long-term anxiodepressive-like consequences of neuropathic pain.** Neuropathic
710 pain induces anxiodepressive-like consequences which disappear in a time-dependent manner.
711 Sciatic nerve injury significantly: decreases the time spent in the lit compartment of the dark–
712 light (DL) box at 8 but not at 2, 11 and 15 Weeks (W) post-surgery (PO) (A), decreases grooming
713 behavior in the splash test at 9, 12 and 14 but not at 3 and16 W PO (B), increases the latency to

feed in the novelty suppressed feeding test (NSF) at 8, 11, 16 but not at 2, 18, 21 W PO (C), increases immobility time at 7, 14, 17 but not at 18, 21 W PO in the forced swimming test (FST) (D). Cuff implanted animals did not show any locomotor activity deficits at Time points (TP) 1, 2 and 3 (E). For a given test, each time point was obtained in an independent set of mice and their corresponding von Frey results are presented nearby (A-D). TP1 corresponds to animals displaying mechanical hypersensitivity but not yet anxiodepressive-like consequences, TP2 corresponds to animals displaying both mechanical hypersensitivity and anxiodepressive-like consequences, TP3 corresponds to animals which recovered from mechanical hypersensitivity but still displayed depressive-like consequences, TP4 corresponds to animals which recovered from both mechanical hypersensitivity and anxiodepressive-like consequences. Data are expressed as mean ± SEM. Numbers in the bars or nearby activity scores indicate the number of animals. *p< 0.05, **p< 0.01, *** p< 0.001. See also Yalcin et al., 2011 for other time point data between 2 W and 9 W PO.

Figure 3. Nerve injury induces ongoing pain. (A) At Time Point (TP) 2, animals displayed mechanical hypersensitivity, anxiodepressive-like behavior and place preference for ongoing pain relief (10 µg clonidine, intrathecal). (B) At TP3, animals recovered from mechanical hypersensitivity, but still displayed anxiodepressive-like consequences and place preference for ongoing pain relief. (C) At TP4, animals recovered from mechanical hypersensitivity and anxiodepressive-like behavior, and ongoing pain is no longer detected. Each TP corresponds to an independent experiment performed in separate sets of mice. Data are expressed as mean ± SEM. Numbers in the bars indicate the number of animals. *p< 0.05. PWT: Paw withdrawal threshold.

736 **Figure 4. Increased ACC single-unit activity.** (A) Illustration of the recording sites in the
737 anterior cingulate cortex (ACC) (dots) on a sagittal and on a frontal plane. The picture on the
738 right illustrates a Pontamine Sky blue dye deposit at the end of the recording. (B) Overview of
739 the development and recovery of different aspects of neuropathic pain. Time frames of recorded
740 animals correspond to 4 phenotypical time points (TP) defined based on previous experiments
741 (Figure 2) and corresponding to the presence or absence of given behaviors. Each recorded
742 animal was tested for mechanical hypersensitivity and anxiodepressive consequences. (C)
743 Example of representative recordings from sham and nerve-injured animals at TP2. (D) Single-
744 unit firing rate and (E) bursting activity are increased at TP2 and TP3 but not at TP1 and TP4. (F)
745 Increased number of action potentials per burst and increased number of bursting cells at TP2.
746 TP1 corresponds to animals displaying mechanical hypersensitivity but not yet anxiodepressive-
747 like consequences, TP2 corresponds to animals displaying both mechanical hypersensitivity and
748 anxiodepressive-like consequences, TP3 corresponds to animals which recovered from
749 mechanical hypersensitivity but still displayed depressive-like consequences, and TP4
750 corresponds to animals which recovered from both mechanical hypersensitivity and
751 anxiodepressive-like consequences. Data are expressed as mean ± SEM. Numbers in the bars
752 indicate the number of cells and animals. *p< 0.05, **p< 0.01, ***p< 0.001. cc: Corpus
753 callosum, LV: Lateral ventricle.

754 **Figure 5. Facilitated pre- and post-synaptic ACC transmission in nerve-injured animals**
755 **displaying depressive-like behaviors.** (A) Samples (top) and summarized results (bottom)
756 showed that the paired-pulse ratios, with recorded intervals of 35, 50, 75, 100 and 150 ms, were
757 decreased in the cuff group compared to the sham group. (B) Samples (top) and summarized
758 results (bottom) of the amplitude and frequency of mEPSCs. Both amplitude and frequency were

759 increased in the cuff group compared to the sham group. (C) Samples (top) and summarized
760 results (bottom) showed that the input-output curve of AMPARs-mediated EPSCs was steeper in
761 the cuff group. However, the I-V curves were not changed. (D) Samples (top) and summarized
762 results (bottom) showed that the input-output curve of NMDARs mediated EPSCs was steeper in
763 the cuff group. The I-V curve in the cuff group differed from that of the sham group. All
764 experiments were performed at TP2 (8-9 weeks after surgery), which corresponds to animals
765 displaying both mechanical hypersensitivity and anxiodepressive-like consequences. $p< 0.05$,
766 $**p< 0.01$. Numbers in bars or near group names indicate the numbers of cells and animals.

767 **Figure 6. Facilitated pre-synaptic but non post-synaptic ACC transmission in nerve-injured**
768 **animals which recovered from mechanical hypersensitivity.** (A) Samples (top) and
769 summarized results (bottom) showed that the paired-pulse ratios, with recorded intervals of 35,
770 50, 75, 100 and 150 ms, were not changed in the cuff group compared to the sham group. (B)
771 Samples (top) and summarized results (bottom) of the amplitude and frequency of mEPSCs.
772 Frequency was increased in cuff group compared to the sham group. (C) Samples (top) and
773 summarized results (bottom) showed that the input-output and I-V curves of AMPAR-mediated
774 EPSCs were not changed in the cuff group. (D) Samples (top) and summarized results (bottom)
775 showed that the input-output curve of NMDAR mediated EPSCs was not different in the cuff
776 group. The I-V curve in the cuff group differed from that of the sham group. All experiments
777 were performed at TP3 (14-16 weeks after surgery), which corresponds to animals that recovered
778 from mechanical hypersensitivity but still displayed depressive-like consequences. $*p< 0.05$.
779 Numbers in bars or near group names indicate the number of cells and animals.

780 **Figure 7. Optogenetic ACC inhibition blocks the aversiveness of ongoing pain and the**
781 **anxiodepressive-like consequences of neuropathic pain.** (A) Representative picture of an

AAV5-CaMKII-eArchT3.0-EYFP site 5 weeks after transfection. (B) Light-evoked effects recorded in the ACC pyramidal neurons of AAV5-CaMKIIa-eArchT3.0-EYFP injected mice. Top: representative trace recorded in the current-clamp mode, note the full inhibition of spikes at all tested luminances; middle: representative trace of light-evoked currents recorded in the voltage-clamp mode; bottom: luminance-response curve of light-evoked currents (n=6); the maximal luminance corresponds to 16 mW. (C) Mechanical hypersensitivity is not affected by ACC inhibition at both Time Point (TP) 2 and TP3. PWT: Paw withdrawal threshold. (D) Optogenetic inhibition of the ACC induces a place preference at TP2 and TP3 in nerve-injured animals (but not in Sham animals) for the chamber in which light was delivered. CPP: Conditioned Place Preference. (E) ACC optogenetic inhibition during the splash test reverses the decreased grooming behavior observed in nerve-injured non stimulated animals at both TP2 and TP3. (F) ACC optogenetic inhibition 5 minutes prior to NSF test blocks the cuff-induced increased latency to feed at TP2. TP 2 corresponds to animals displaying both mechanical hypersensitivity and anxiodepressive-like consequences, TP 3 corresponds to animals which recovered from mechanical hypersensitivity but still displayed depressive-like consequences. For the CPP, Splash and NSF experiments, the laser stimulation used was continuous green light (520 nm) for 5 min at 16mW. Data are expressed as mean ± SEM. Numbers in the bars indicate the number of animals. *p< 0.05, **p< 0.01., ***p<0.001 MC: motor cortex.

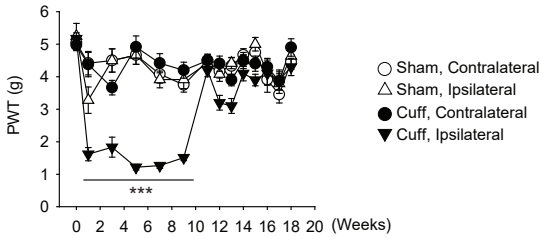

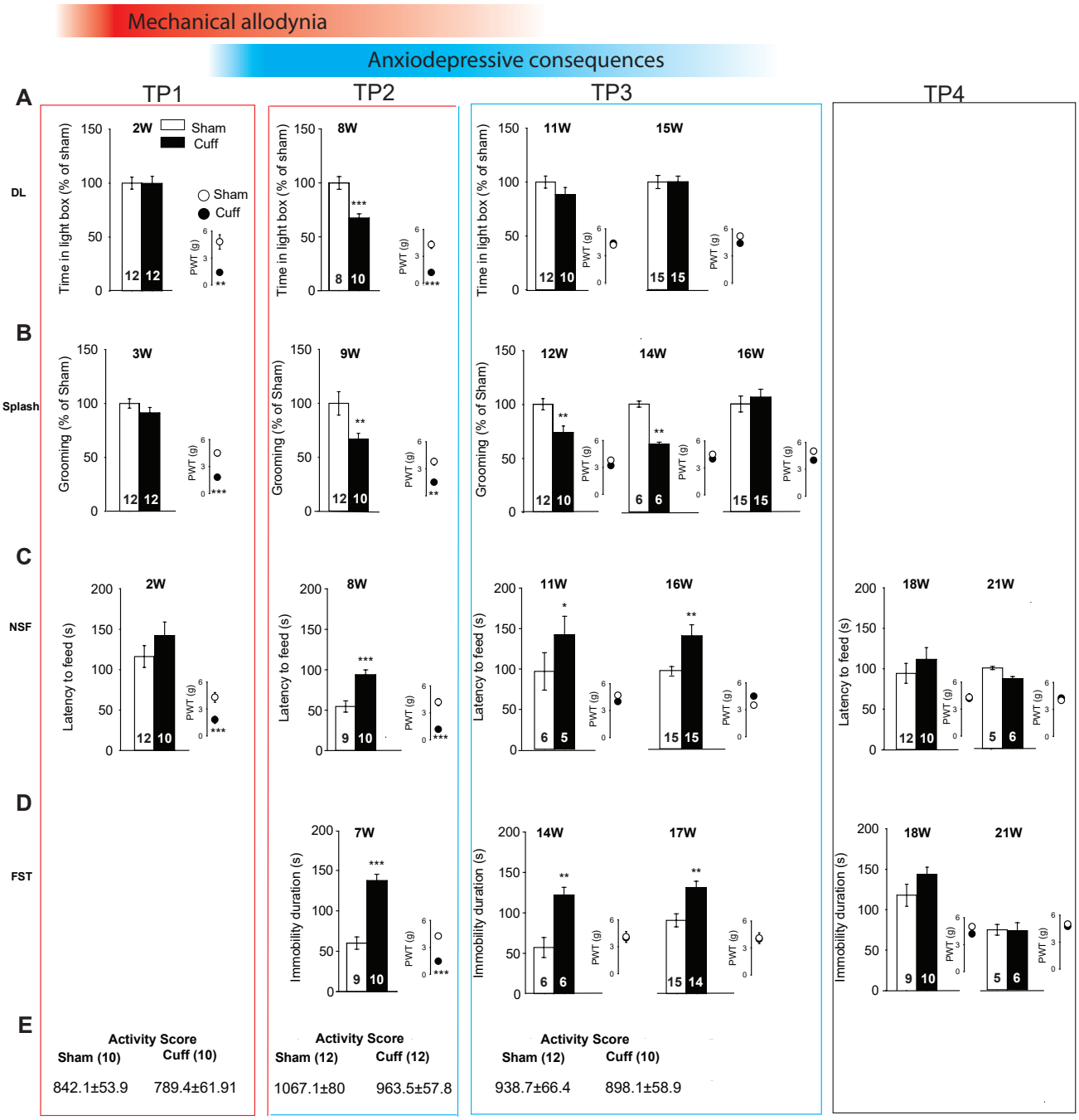

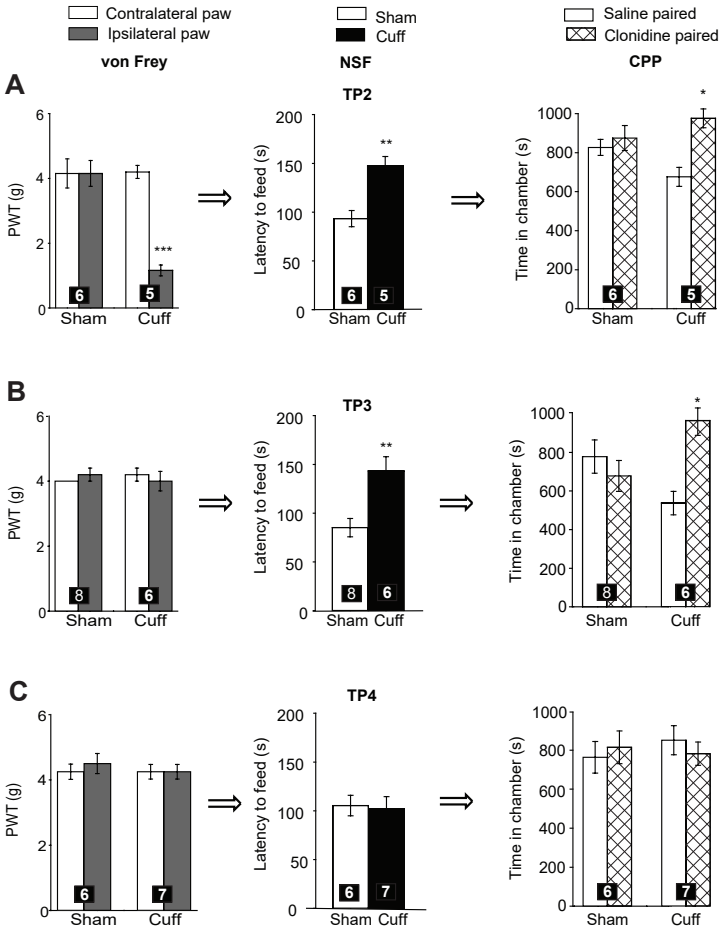

A

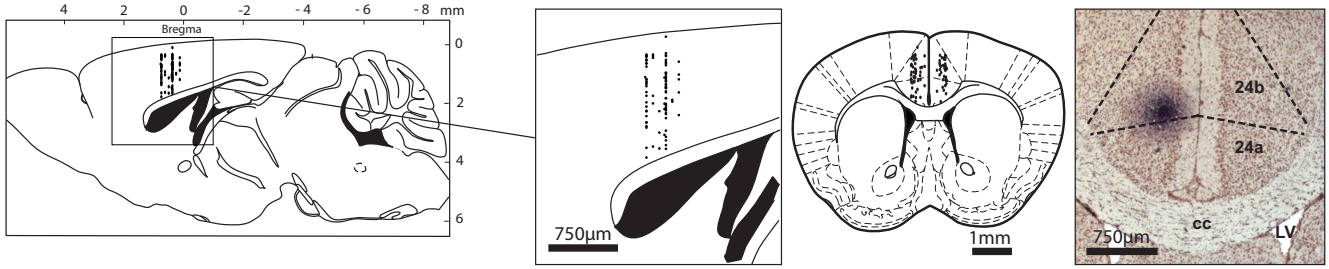

B

	TP1	TP2	TP3	TP4
Anxiety-like behavior	N	Y	N	N
Depression-like behavior	N	Y	Y	N
Mechanical hypersensivity	Y	Y	N	N

C

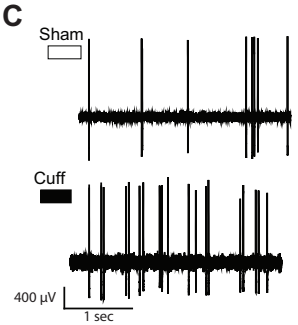

D

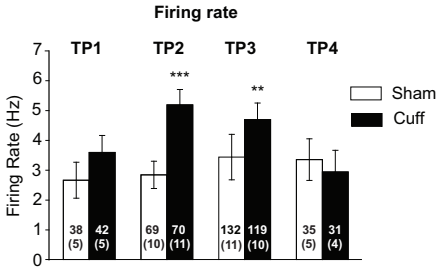

E

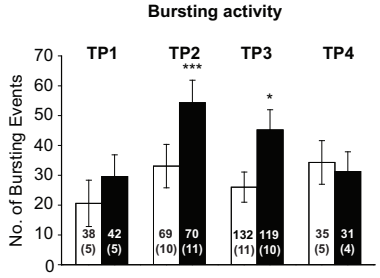

F